Bone

ELSEVIER

Available online at www.sciencedirect.com

SciVerse ScienceDirect

Official Journal
International Bone
& Mineral Society

IBMS

(This is a sample cover image for this issue. The actual cover is not yet available at this time.)

Contents lists available at ScienceDirect

Bone
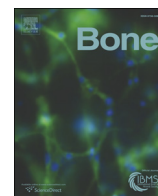
Full Length Article

Open source software for semi-automated histomorphometry of bone resorption and formation parameters

Rob J. van 't Hof [a,*], Lorraine Rose [b,1], Euphemie Bassonga [a,2], Anna Daroszewska [a]

[a] Institute of Ageing and Chronic Disease, University of Liverpool, United Kingdom
[b] Institute for Genetics and Molecular Medicine, University of Edinburgh, United Kingdom

A B S T R A C T

Micro-CT analysis has become the standard method for assessing bone volume and architecture in small animals. However, micro-CT does not allow the assessment of bone turnover parameters such as bone formation rate and osteoclast (OC) number and surface. For these crucial variables histomorphometric analysis is still an essential technique. Histomorphometry however, is time consuming and, especially in mouse bones, OCs can be difficult to detect. The main purpose of this study was to develop and validate a relatively easy and rapid method to measure static and dynamic bone histomorphometry parameters. Here we present the adaptation of established staining protocols and three novel open source image analysis packages: TrapHisto, OsteoidHisto and CalceinHisto that allow rapid, semi-automated analysis of histomorphometric bone resorption, osteoid, and calcein double labelling parameters respectively. These three programs are based on ImageJ, but use a relatively simple user interface that hides the underlying complexity of the image analysis.

1. Introduction

Micro-CT analysis has become the standard method for assessing bone volume and architecture in small animals. However, micro-CT does not allow the assessment of bone turnover parameters such as bone formation rate and osteoclast (OC) number and surface. For these crucial variables histomorphometric analysis is still an essential technique. Several attempts have been made in the past to produce software that will automate bone histomorphometry. However, many of these programs are now obsolete and based on hardware and software that is no longer accessible. Two widely used commercial packages are available: Osteometrics Osteomeasure and Bioquant Osteo. Osteometrics Osteomeasure is largely based on manual tracing of the bone surfaces, while the Bioquant Osteo package uses semi-automated procedures. A drawback of both packages is that they are relatively expensive, and may need specific imaging hardware.

Over the past few years the free and open source image analysis package ImageJ developed at the NIH by Dr. W. Rasband has been established as one of the leading software packages for image analysis,

especially in microscopy [1]. It is a modular system which allows for extension of its capabilities by plug-in modules. It has attracted a wide and active user-base, and this community has contributed a large number of plug-ins, making ImageJ one of the most comprehensive image analysis packages. ImageJ is written in Java, which allows the software to run on any operating system which supports Java, and this currently includes Windows, MacOSX and Linux. Although ImageJ is highly functional, its user interface can be confusing for non-expert users. However, the ImageJ core package and the plugins can be used as imaging libraries in stand-alone programs. We have used this approach to develop three Java-based programs for semi-automated bone histomorphometry, providing data according to the guidelines published by the ASBMR [2,3]. These free and open source programs provide a cost effective alternative to commercial packages for the measurement of the major bone histomorphometry parameters. Furthermore, because they are open source, the algorithms and calculations used in the software can be verified, and the software can be relatively easily adapted to the specific needs of individual users or applications. The main purpose of this study was to develop and validate a relatively easy and rapid method to measure static and dynamic bone histomorphometry parameters.

2. Methods and materials

All standard chemicals, solvents and dyes were from Sigma (Poole, UK) unless otherwise indicated.

---

* Corresponding author at: Institute of Ageing and Chronic Disease, University of Liverpool, 6 West Derby Street, Liverpool L7 8TX, United Kingdom.
E-mail address: r.vanthof@liverpool.ac.uk (R.J. van 't Hof).
[1] Current address: Centre for Cardiovascular Research, University of Edinburgh, United Kingdom.
[2] Current address: Centre for Orthopaedic Research, University of Western Australia, Australia.

2.1. Tissue preparation and embedding

Male C57/Bl6 mice (9 weeks old) were injected intraperitoneally with a calcein solution (10 mg/kg) as described by Erben [4], 5 days and 2 days before euthanizing. Mouse L5 vertebrae were dissected, fixed for 24 h in neutral buffered formalin, and stored in 70% ethanol. Before embedding, the samples were dehydrated through an alcohol series and two changes of Xylene at 4 °C using a Leica EM TP6 tissue processor. The samples were infiltrated at 4 °C under vacuum with a mixture of 88.99% methyl methacrylate (TAAB, UK), 10% di-butyl phthalate (TAAB, UK), 1% Perkadox 16 (Akzo Nobel, Deventer, the Netherlands) and 0.01% Novoscave (Novochem, Reinach, Switzerland) for 7 days. After infiltration, the samples were placed in the wells of Teflon embedding blocks filled with the infiltration mixture, the wells sealed with air-tight lids, and the blocks left to polymerise in a water bath at 30 °C for a minimum of 18 h. After polymerisation was complete, the lids were removed and embedding rings were attached using Historesin (Leica, UK). Blocks were left to harden for at least 2 days before sectioning at 5 μm using a Leica RM2265 motorised microtome fitted with a tungsten steel D-profile knife. The sections were mounted on polylysin coated microscopy slides (Polysciences, Germany), covered with kissol film (TAAB, UK) and placed under pressure in a slide-press (TAAB, UK) at 37 °C for at least 48 h. A human iliac crest biopsy obtained during surgery on a female adolescent patient investigated for osteoporosis reported previously [5] was fixed, processed and cut according to the same protocol.

2.2. Osteoclast staining

Osteoclasts in the murine vertebral body of L5 vertebra were identified by tartrate resistant acid phosphatase (TRAcP) staining, and bone was stained using Aniline Blue. This procedure is an adaptation of the method described by Chappard et al. [6]. Briefly, sections were deplasticised in 3 changes of 2-methoxyethyl acetate (MEA), cleared in two changes of Xylene and taken through a decreasing alcohol series to water. The sections were incubated at 37 °C for up to 2 h in a staining solution of naphtol ASTR-phosphate (1.4 mg/ml) and fast red (1.4 mg/ml) in a 0.2 M actetate buffer (Ph 5.2) containing 100 mM sodium tartrate. After the TRAcP stain the sections were washed in two changes of water and counterstained for 15 min using 0.33 g/l Aniline Blue and 6 g/l phosphotungstic acid in water, and briefly rinsed in two changes of water. The sections were either coverslipped using Apathy's serum, or air-dried, dipped in Xylene and coverslipped using DPX.

2.3. Counterstain for calcein double label analysis

For analysis of calcein double labels, sections were stained with either a modified Aniline Blue stain, which lacks phosphotungstic acid, or Calcein Blue. Briefly, sections were stained without deplastification for 10 min in Aniline Blue in water (0.6 g/l), washed twice briefly in water, dehydrated through an alcohol series, cleared in Xylene and coverslipped using DPX or Eukit.

For the Calcein Blue stain, sections were stained without deplastification for 3 min in 0.1% Calcein Blue pH 8. The sections were washed twice in water, dehydrated through an alcohol series, cleared in Xylene and coverslipped using Eukit. This staining protocol leads to bright blue fluorescence of mineralised tissue.

2.4. von Kossa-van Giesson staining

Sections were deplasticised in 3 changes of MEA, cleared in two changes of Xylene and taken through a decreasing alcohol series to water. Sections were stained for 2 min in a 1.5% aqueous solution of silver nitrate in the dark, washed in water and the stain developed in a 0.5% hydroquinone solution for 2 min and washed in water. The sections were counterstained using van Gieson's stain (TAAB, UK) for 3 min and

washed in water. Finally, the stained sections were dehydrated through an alcohol series, cleared in xylene and coverslipped using DPX. This stain results in mineralised tissues being stained black and osteoid purple-red.

2.5. Image acquisition

Sections were imaged on a Zeis Axioimager microscope fitted with a QImaging Retiga 4000 camera, which was calibrated using a stage micrometer. Using a macro in the FIJI distribution of ImageJ (available from http://fiji.sc/Fiji), multiple images of a section were captured using the Qcam plugin from Qimaging and combined with the aid of the 2D and 3D stitching plugins developed by Stephan Preibisch [7]. As the QImaging camera does not provide built-in shading correction, shading correction of the images was performed using the shader plugin, and extended depth of field was performed using the stack focuser plugin developed by Michael Umorin (http://rsb.info.nih.gov/ij/plugins/stack-focuser.html). The shading correction was slightly modified by preventing overflow of 8-bit images through capping the maximum of the corrected intensity at 255, and for colour images by converting to the HSB colour space and only correcting the brightness, leaving the hue and saturation unchanged. The stack focuser plugin was modified to take advantage of multi-core processors by implementing multithreading.

Alternatively, sections were imaged using an Olympus Dotslide motorised microscope system. Colour imaging of TRAcP and von Kossa-van Giesson stained sections used a 10× lens and the extended depth of field option provided by the Olympus software. The calcein - calcein blue stained sections were imaged using the monochrome camera and a 20× lens. The Olympus system performs automatic shading correction, and therefore it was not necessary to perform shading correction in ImageJ on these images. As the Olympus software does not provide the option of extended depth of field imaging for fluorescence images, sections were imaged as a 3D stack (9 planes at 10 μm spacing) and the extended depth of field image was created using the stack focuser plugin in Fiji as described above.

2.6. Software development

Analysis software was written in Java using the Netbeans IDE (version 8.1). Both the source code and the final programs can be downloaded from https://www.liverpool.ac.uk/ageing-and-chronic-disease/bone-hist.

ImageJ was used as an image analysis library, and the ImageJ Image processor class was used for image handling throughout all three programs. Several additional plug-ins available in the public domain were used. The Local Thickness plugin from Bob Dougherty (OptiNav Inc., http://www.optinav.com/Local_Thickness.htm), and the Skeletonise3D and AnalyzeSkeleton plugins from Ignacio Arganda-Carreras [8] were used for the osteoid and double label width and length measurements. The Principal Curvatures plugin by S. Preibish (http://fly.mpi-cbg.de/~preibish/software.html#Curvatures) was used for detection of calcein labels.

For ease of use and speed optimisation, several image analysis functions were adapted or developed specifically for this software. These include multi-threaded methods for thresholding of images, hysteresis thresholding, a binary erode-reconstruct algorithm, filtering of binary clusters by size, and a number of routines for creating, measuring and managing image object sets. Furthermore, a custom image display class was developed that allows the simultaneous display and manual editing of several coloured binary overlays.

2.7. Reproducibility and validation

The intra- and inter-observer variation of the measurements produced through TrapHisto, OsteoidHisto and CalceinHisto were assessed.

The intra-observer variation was assessed by comparing the analyses of the same samples carried out on three consecutive days by one observer (RvH). The inter-observer variation was assessed by comparing the analyses of the same samples carried out by three observers independently. Results from the ImageJ based software packages were compared to results obtained by analysing the same images using Bioquant Osteo II version 8.40.20MIR.

3. Results

3.1. Software

We developed three separate programs, TrapHisto, OsteoidHisto and CalceinHisto. The three programs measure bone resorption parameters from TRAcP-stained sections, basic bone architecture and osteoid parameters from von Kossa-van Giesson stained sections, and bone formation parameters from calcein double labels respectively. The resulting programs use the power of ImageJ in combination with a much simplified, integrated user interface and an image display module which allows the non-destructive and editable overlay of multiple datasets, such as bone surface, resorption surface and osteoid markers (Fig. 1). The end user is completely shielded from the ImageJ plug-ins that underlie the programs, and is presented with a series of instructions and tool panels to guide them through the analysis. The interface tries to minimise the use of image analysis jargon such as "binary close" or "erode-reconstruct", using easier to understand descriptions such as "close cracks" and "remove small particles" instead. Bone histomorphometry regularly requires human judgement to correct for artefacts in the samples such as cracks or poor staining. The software therefore allows manual editing of all automatically detected features.

3.2. Resorption analysis using the TrapHisto program

The Aniline Blue and TRAcP stains bone tissue blue and osteoclasts red respectively (Fig. 2A), a result which is relatively easily analysed
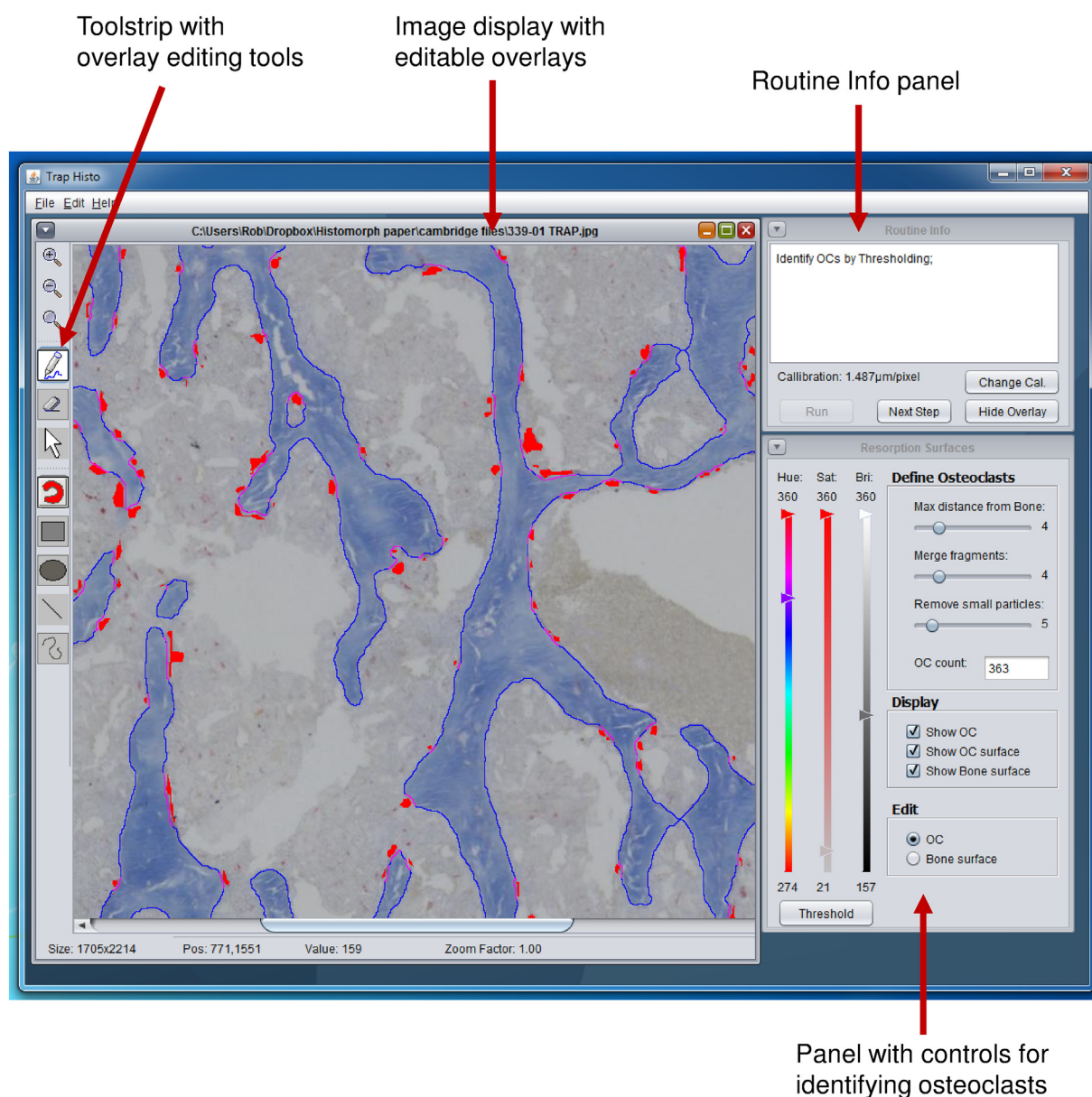
Fig. 1. User interface of the TrapHisto program. Screen shot showing detail of an Aniline Blue and TRAcP stained section of a mouse vertebra during analysis with the TrapHisto program. The interface is relatively simple consisting of an image display window with an overlay editing toolbox, an info panel for messages to the user and buttons to set the pixel size and control progression through the analysis routine, and a panel with controls specific to the current step in the analysis routine.

Fig. 2. Resorption analysis using the TrapHisto program. Sections of mouse L5 vertebral bodies were stained for TRAcP, counterstained with Aniline Blue, and imaged at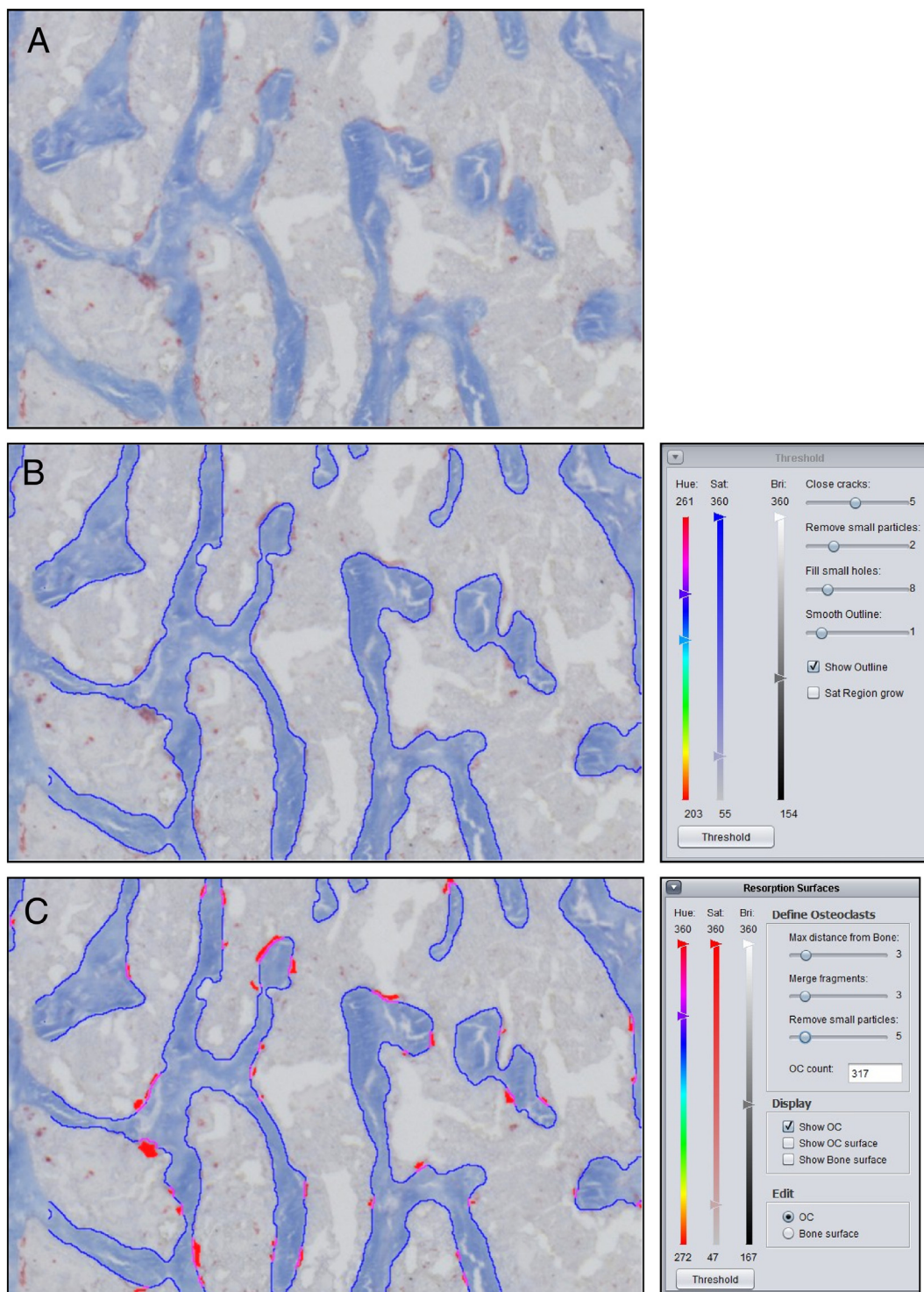 a resolution of 1.4 μm before analysis using the TrapHisto program. Panels A–C show screenshots from the analysis. A: Detail of an Aniline Blue and TRAcP stained section of a mouse vertebra. B: Identifying Bone: The Aniline Blue stained bone is identified using colour thresholding. Cracks and holes are removed using binary opening and closing (command 'close cracks'). Small particles are removed using an erode-reconstruct algorithm (command 'remove small particles'). Remaining defects can be edited manually. The bone surface is outlined in blue. C: Identifying osteoclasts: The TRAcP stained osteoclasts are identified using colour thresholding. Objects too far removed from the bone surface are deleted and fragments in close proximity fused using binary closing. (For interpretation of the references to colour in this figure legend, the reader is referred to the web version of this article.)

using simple thresholding. The DPX coverslipping method leads to improved optical clarity and avoids the slow fading of the Aniline Blue, which slowly dissolves in the Apathy's serum. However, the air drying necessary for this method can lead to formation of cracks in the tissue. If images can be captured within a reasonable time frame (up to 3 days), the Apathy's serum method is preferred.

The images were captured using a 10× objective lens on a Zeiss AxioImager microscope fitted with a QImaging Retiga 4000R camera, with ×2 binning. This combination allows the capture of a large portion of a mouse vertebral body, femur or tibia section at sufficient resolution (resulting pixel size of 1.4 μm) for analysis. However, multiple images are still required to capture the full area required for histomorphometric

analysis. To this end multiple images were acquired and stitched together using the 2D stitching plugin in the FIJI distribution of ImageJ. A small macro was developed to automate this process and to apply shading correction and extended depth of view.

After opening the image to be analysed, the first step in the TrapHisto analysis is to identify the region of interest manually, using the overlay drawing tools. Next, the bone tissue is identified by an interactive threshold in the hue-saturation-brightness (HSB) colour space (Fig. 2B). An option allows the user to use a hysteresis threshold for the saturation band. This grows seed areas defined by an inner threshold to those defined by the outer threshold, and can be helpful in cases where the Aniline Blue stain has started to fade. Small sectioning artefacts such as cracks can be removed using simple binary close ('close cracks') and hole-fill operations. Small particles in the image are removed using an erode-reconstruct algorithm. Any remaining artefacts can still be corrected by manual editing of the binary overlay.

Next, the osteoclasts are identified using an HSB threshold operation (Fig. 2C). As osteoclasts are normally located on the bone surface, the user can specify a maximum distance from the bone surface. TRAcP positive fragments that are in close proximity are likely to be part of a single osteoclast. A binary closing operation can merge these fragments into single objects. Any remaining small particles can be easily removed using a slider that specifies the minimum size for an osteoclast in pixels. Fig. 2C shows a section with osteoclasts identified in red, bone resorption surface in magenta and bone surface in blue. The calibrated results are saved as an Excel compatible document in *.csv format.

3.3. Osteoid analysis using the OsteoidHisto program

Most mouse bone sections show very little osteoid, unless there is a distinct defect in mineralisation. To test the OsteoidHisto program we therefore used an adolescent human iliac crest biopsy, which shows abundant osteoid seams. Sections were stained using von Kossa-van Giesson to enable identification of mineralised tissue (black) and osteoid (purple-red). Von Kossa-van Giesson stained sections were imaged using a 10× objective as described above. The software is very similar to the TrapHisto program, however, the bone is identified using a standard Red-Green-Blue colour threshold as this is more efficient at identifying the black von Kossa stain (Fig. 3A). Next the osteoid is identified using thresholding in the HSB colour space (Fig. 3B). The osteoid thickness is calculated as a weighted mean of the osteoid seams in the image using the LocalThickness plugin. This plugin performs a circle fitting algorithm to measure object thickness as described by Hildebrand et al. [9].

3.4. Calcein double label analysis using the CalceinHisto program

A standard Aniline Blue stain destroys the calcein labels, however, omitting the phosphotungstic acid from the stain preserves these with acceptable staining of the bone tissue allowing identification by thresholding (Fig. 4A and B). Image contrast can be increased by the use of a red filter during image capture. The samples were captured using a macro similar to the one described for the TRAcP analysis. However, two images were captured for each field: a bright field image for the Aniline Blue stain and a fluorescence image (using a standard FITC filter set) for the calcein labels, and stitched together using the 3D stitching plugin. This results in a stack with the first image being the Aniline Blue stain, and the second the fluorescent calcein label image. The resolution of the system using a 10× objective was not sufficient for the accurate measurement of the double label distance, and the sections were therefore measured using a 20× objective and a pixel size of 0.35 μm. Although the adapted Aniline Blue stain results in reasonable staining of mineralised tissue, poorly mineralised bone is not well stained. The alternative staining method using Calcein Blue leads to intense blue fluorescence of bone tissue with negligible background using a standard DAPI filter-set (Fig. 4C and D). The Calcein Blue images are

more straightforward to analyse and were therefore used for the final analysis.

Similar to the TrapHisto and OsteoidHisto programs, the first step of the analysis routine is the identification of the area to be analysed using the overlay drawing tools. The next step is the identification of bone using thresholding, with an option for using hysteresis thresholding for improving detection in poorly stained specimens (Fig. 5A). The procedure is similar to that described for the TRAcP analysis and offers similar options. After the identification of the bone, the software attempts to automatically detect the calcein labels (Fig. 5B). A standard threshold of the fluorescence image resulted in suboptimal identification of the labels. At a setting which was sensitive enough to pick up weak labels, many of the stronger double labels would merge into a single label. Therefore, a protocol was developed based on line detection using the Eigen values of the Hessian matrix. An existing ImageJ plugin (Principal Curvatures by S. Preibish, see methods), was modified and adapted for the detection of bright, line-like structures on a dark background, and the processing speed was improved by multithreading the procedure. Thresholding the resulting image avoids the problems with the merging of double labels while still being able to identify weakly stained labels, and the standard settings work well for most of the images tested. The centreline from the threshold result is determined using a skeletonise operation using the Skeletonize_3D plugin [8]. Small side branches are pruned while preserving the main path using the AnalyzeSkeleton plugin [8]. Finally in this stage, the centre line can be smoothed out. This is accomplished by performing a binary dilation followed by a skeletonise operation. The resulting overlay can still be manually edited.

Once the calcein labels have been identified, these are classified as either single or double labels in the next step (Fig. 5C). This step uses two parameters. The first (maximum double label distance) is used in a binary close operation. The width of the objects in the resulting binary image is then calculated using the LocalThickness plugin. A second parameter (minimal double label thickness) is used to determine a threshold for the local thickness result image, removing areas where the thickness does not meet the minimal thickness criteria. Any labels not identified in this procedure as double labels are classified as single labels. The labels are projected onto the closest bone surface, and the length of the resulting label surfaces is calculated using the AnalyzeSkeleton plugin. The overall double label distance is calculated as a weighted average thickness of all individual pixels that make up the centre lines of the double labels. The thickness at each point is defined as the largest circle that can be fitted inside the double label that has that point as its centre. The data are exported to an Excel compatible file for further analysis.

Although most of the labels are detected correctly, under certain circumstances labels may fail to be classified properly. When several single labels are situated closely together, the software may classify these as a single double label (Fig. 6A), requiring manual editing of the label image. Labels that are cut at an oblique angle often pose problems by not being properly detected, leading to miss-classification of single labels as double labels, or incorrect detection of the centreline of the label (Fig.6B). These errors can be corrected manually either at the label-detection stage, or at the classification stage.

3.5. Image capture using an automated microscope system

The semi-automated analysis substantially speeded up the histomorphometric analysis process. However, the image capture, especially of relatively large sections such as mouse lumbar vertebrae or human bone biopsies, was still a relatively time consuming task. To increase the throughput in image capture, we used a fully automated microscope (Olympus Dotslide) equipped with a robotic slide changer and both colour and high sensitivity monochrome cameras.

The TRAcP-Aniline Blue and von Kossa-van Giesson stained sections were imaged using the colour camera at 10× magnification (0.6 μm pixel size). The colour imaging allowed the use of a robotic slide loader,
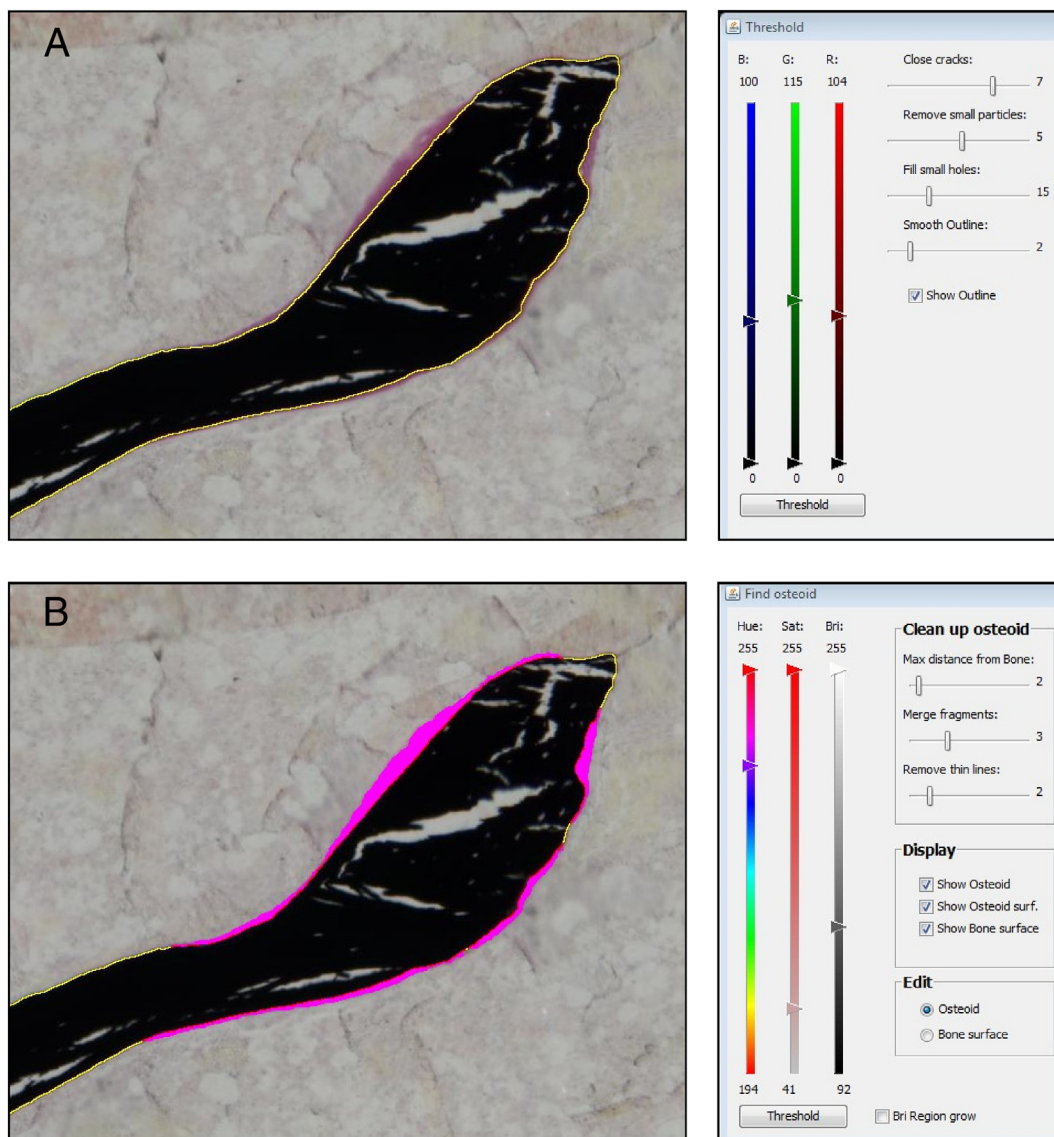
Fig. 3. Osteoid analysis using the OsteoidHisto program. Sections of an adolescent human iliac crest biopsy were stained using von Kossa-van Giesson, and imaged using an Olympus Dotslide automated microscopy system at a final resolution of 1.2 μm before analysis using the OsteoidHisto program. Panels A and B show screenshots from the analysis. A: The von Kossa stained bone is identified using colour thresholding. Cracks and holes are removed using binary opening and closing. Small particles are removed using an erode-reconstruct algorithm. The mineralised bone is outlined in yellow. B: The van Gieson stained osteoid is identified using colour thresholding. Osteoid like objects too far removed from the bone surface are deleted and fragments in close proximity fused using binary closing. Thin osteoid seams are removed using an erode-reconstruct procedure. The osteoid seams are labelled in magenta. (For interpretation of the references to colour in this figure legend, the reader is referred to the web version of this article.)

and after an initial 1 h setup, this allowed the fully automatic and unattended capture and stitching of 50 slides with three sections each within half a day. The images were scaled down a factor 2 using ImageJ for a final resolution of 1.2 μm/pixel.

The calcein double label-calcein blue sections were imaged using the monochrome camera. The robotic slide loader is not available for fluorescence microscopy on this system. However, imaging a section of a mouse vertebral body at 20× magnification (0.3 μm pixel size) took approximately 5 min using the automated microscope as opposed to 20–30 min using a manual microscope.

3.6. Reproducibility

A selection of sections was analysed on 3 separate days by one observer (RvH) to determine reproducibility of the measurements, and the same sections were also analysed by 2 additional observers (LR and AD) to determine intra-observer variation.

Reproducibility of the results for the TrapHisto program was generally good, with intra-observer coefficient of variance (CV) in the range of 1–4%, and inter-observer CV (3 observers) in the range of 2–5% for resorption parameters (Table 1), with the exception of Oc.S/BS which showed a CV of 8% for one of the samples.

Measurements of bone architecture using the OsteoidHisto program were highly reproducible as well with inter-observer CV% of 2–4% for BV/TV, BS/BV, Tb.Th and O.Th (Table 2). However, OS/BS and OV/BV showed higher variability with CV% between 8 and 12%.

Bone formation parameters measured using CalceinHisto (Table 3) showed very good reproducibility for the mineral apposition rate (CV 1–4%). The mineralising surface per bone surface and bone formation rate showed considerably higher variance with CV values of 8–10%, even for intra-observer CV. This may be partially due to the presence of very faint labels which may be frequently missed.

Finally, we compared the results from the suite of ImageJ-based programs presented here with measurements performed on the same images using Bioquant Osteo (Table 4). One considerable difference
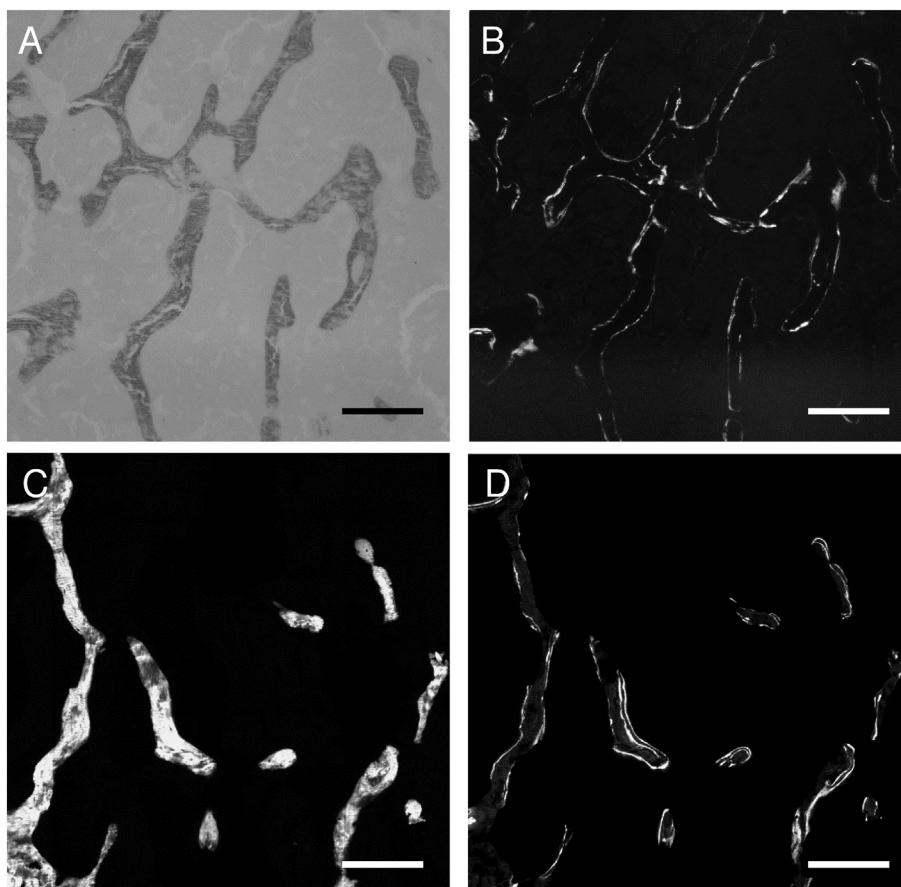
Fig. 4. Bone counter stains that preserve calcein double labels. A: Detail of a mouse bone sample stained with the adapted Aniline Blue stain, captured using a monochrome camera. B: The specimen in panel A was subsequently imaged by fluorescence microscopy showing good preservation of calcein labels. C: Mouse bone specimen stained using the calcein blue method and imaged by fluorescence microscopy using a DAPI filter set. Staining shows very good contrast of mineralised tissue and virtual absence of background. D: Calcein labels of the specimen in panel C. The scale bars in panels A–D indicate 100 μm.

between the ImageJ based programs and the Bioquant Osteo version used, is the amount of time required for performing the analysis, with the Bioquant Osteo software requiring substantially longer. This was for a large part due to the requirement to manually draw in features such as resorption surfaces and calcein labels. In addition, the user interface of Bioquant Osteo is considerably more complex and takes substantially longer to get familiar with. The results for basic histomorphometric measurements such as BV, TV and BS and measurements directly derived from these such as BV/TV, BS/BV and Tb.Th show very little, typically less than 5%, difference between the ImageJ based programs and Bioquant Osteo. Measurements that require manual input in Bioquant Osteo, such as Oc.S, OV, O.Th and MAR show considerably higher levels of variation, with the ImageJ based measurements generally resulting in higher values. Analysing the MAR of the same test image manually using ImageJ gave a MAR of 2.03 μm/day, a value higher than the results obtained using Bioquant Osteo (1.23 μm/day) and CalceinHisto (1.71 μm/day).

4. Discussion

The method for performing bone histomorphometry described here is relatively easy and rapid. For well stained, good quality sections, analysis can be performed in approximately 5–10 min/section. Especially for the TrapHisto and OsteoidHisto programs, this time is further reduced for subsequent slides from the same staining batch, as the thresholds for the first section can normally just be reapplied. Poor quality specimens can take considerably longer due to the requirement for extensive manual editing. The traditional method for analysing calcein double labels was especially time consuming, especially for large specimens such

as murine lumbar vertebrae, due to the time spent on the outlining of the calcein labels manually. Semi-automated detection of the calcein labels resulted in a substantial decrease in time required for the analysis. Novel methods to improve the classification of single and double labels are currently under development. If successful, this should further reduce the amount of time required for manual editing, and therefore analysis time.

The results obtained by using our programs are highly reproducible. However, certain measurements are somewhat more susceptible to user interpretation such as the thresholding of osteoid, as the border between calcified bone and osteoid is distinctly fuzzy. The identification of faint calcein labels also showed considerable variation between operators. These factors can lead to higher CV levels of 8–10%, although this is still considerably lower than the variance observed within treatment groups. In a recent transgenic mouse study we performed, we found CV levels of resorption and formation parameters within treatment groups in the 20–30% range (data not shown). In two papers describing early semi-automated histomorphometry programs [10,11] similar operator-dependent variance was found, and the paper by Juvin et al. [10] noted considerable variance especially in osteoid parameters with a CV up to 12%. A more recent paper by Tong et al. [12] using Bioquant Osteo to perform histomorphometry on human femoral neck samples found intra-observer CV levels of up to 6% and inter-observer levels of up to 16% for most of the parameters measured, levels comparable to those observed using our ImageJ based histomorphometry software. However, they noted that variance in osteoid measurements could be considerably higher with a CV of up to 88% [12]. Therefore, to minimise variance it is advisable for all the samples in a study to be analysed by a single operator, if possible with full validation by a second operator.
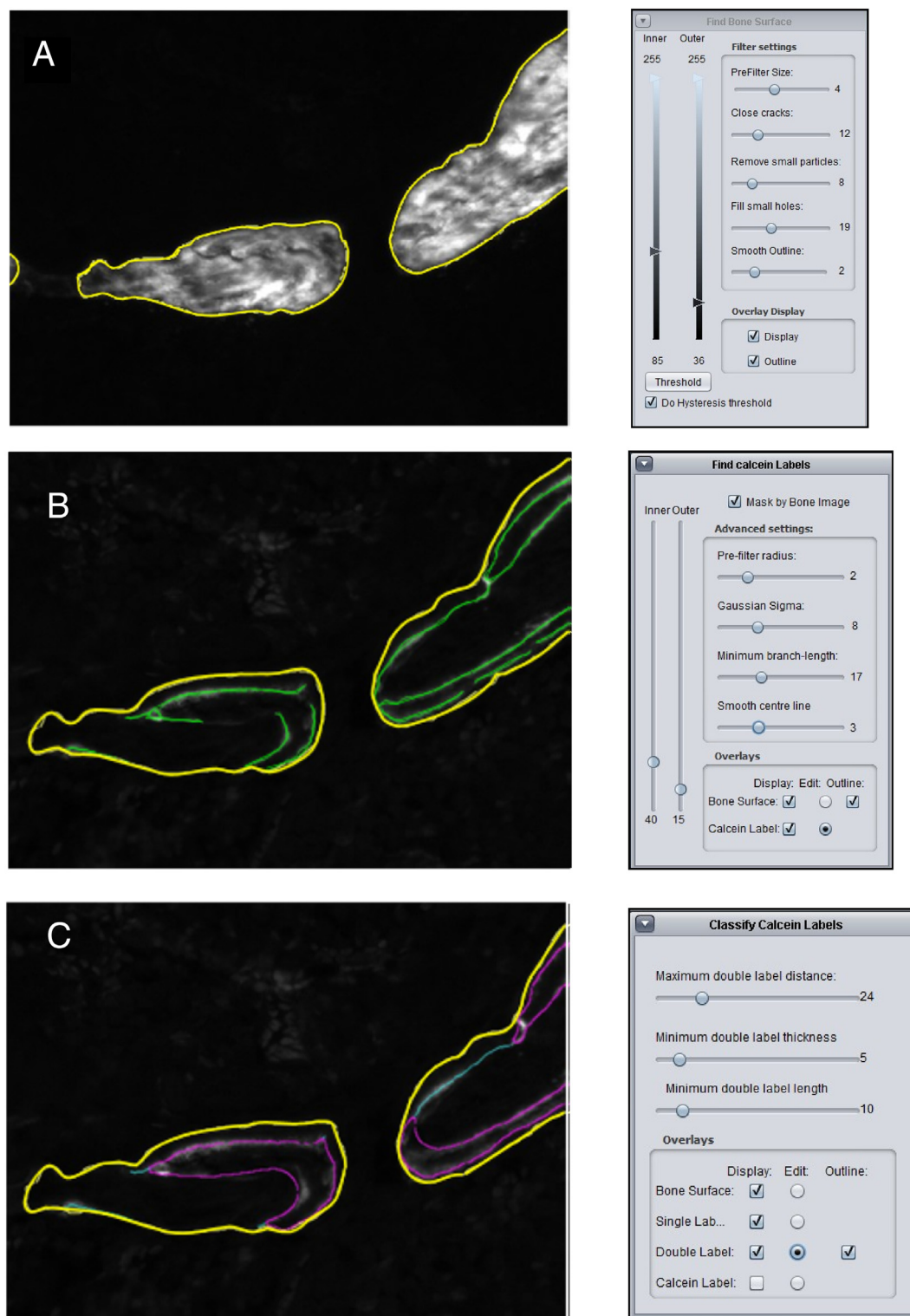
Fig. 5. Analysis of calcein double labels using the CalceinHisto program. Sections of mouse L5 vertebral bodies were counterstained with calcein blue, and imaged using a Zeiss AxioImager fluorescence microscope at a resolution of 0.35 μm before analysis using the CalceinHisto program. Panels A–C show screenshots from the analysis. A: The calcein blue stained bone is identified using thresholding. Cracks and holes are removed using binary opening and closing. Small particles are removed using an erode-reconstruct algorithm. The bone surface is shown as a yellow outline. B: The calcein labels are detected using an algorithm identifying line-like structures in the image. The centre lines of the labels are indicated by a green line. C: The labels are classified as double- or single labels using a combination of binary closing and thresholding of local thickness of the closed binary. Single labels are identified by a light blue centre line, the double labels by a magenta outline. (For interpretation of the references to colour in this figure legend, the reader is referred to the web version of this article.)

Comparison with Bioquant Osteo showed that values of basic parameters were very similar between the software packages. However, some parameters showed considerable discrepancies. This may be partially due to the fact that the ImageJ based programs identify the features underlying these measurements semi-automatically, as compared to a manual operator who can miss features and be less accurate. The most pronounced difference was in the measurements of the MAR and the osteoid thickness, with CalceinHisto and OsteoidHisto
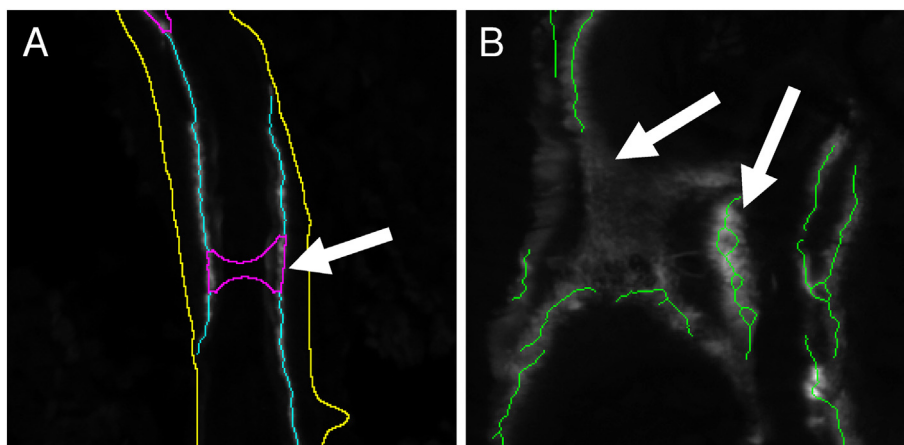
Fig. 6. Problematic situations in CalceinHisto requiring manual correction. Panels A and B show screenshots from situations where CalceinHisto fails to correctly identify labels automatically. A: In some cases, single labels that are relatively close together can be erroneously identified as a double label. The arrow indicates such an error. Yellow: outline of mineralised tissue; blue: single label; magenta: double label. B: Labels cut at an oblique angle are sometimes not identified, or the algorithm produces branching centre lines. (For interpretation of the references to colour in this figure legend, the reader is referred to the web version of this article.)

measurements 39% and 56% respectively larger than Bioquant Osteo. This may be due to two factors. First, Bioquant Osteo requires the user to draw the centre lines of the calcein labels manually, which is a notoriously difficult and time consuming task. CalceinHisto, in contrast, computationally determines the centreline. Secondly, object thickness is measured using very different methods. CalceinHisto and OsteoidHisto measure the thickness of objects using a circle-fitting method which is a 2-dimensional implementation of 3D sphere fitting as used in thickness calculations in μCT scans [9]. Our adaptation of this method determines the local thickness at a pixel within the object as the largest circle that can be fitted within the object that has this pixel as its centre

point, and then calculates the average thickness by averaging the local thickness measurements from all pixels along the centre line of the object. Bioquant Osteo, on the other hand, determines the thickness by drawing lines at pre-set intervals along the object at a 90° angle to the main axis of the object. Interestingly, a paper on an early semi-automated system for bone histomorphometry also found consistently higher values for automated measurements of MAR and osteoid parameters than a manual method [10].

Although the software described here will even run on older PCs with 2GB of RAM, large images require the use of a 64-bit operating system, such as Windows 7 or 10, with 8GB of RAM. Any modern PC will

Table 1
TrapHisto, reproducibility of measurements.

	Oc.S/BS	N.Oc/BS	N.Oc/BV	N.Oc/TV
Observer 1	%	mm^{-1}	mm^{-2}	mm^{-2}
339-01 TRAP	23.14	8.55	415.41	112.40
339-01 TRAP	23.84	8.68	406.80	114.80
339-01 TRAP	22.59	8.30	396.19	109.79
Average	*23.19*	*8.51*	*406.13*	*112.33*
SD	*0.63*	*0.19*	*9.63*	*2.51*
CV%	**2.70**	**2.27**	**2.37**	**2.23**
345-01 TRAP	30.00	9.63	404.50	109.21
345-01 TRAP	29.44	9.61	410.96	108.16
345-01 TRAP	27.81	9.39	391.74	107.86
Average	*29.08*	*9.54*	*402.40*	*108.41*
SD	*1.13*	*0.13*	*9.78*	*0.70*
CV%	**3.91**	**1.39**	**2.43**	**0.65**
Inter observer				
339-Obs 1	22.59	8.30	396.19	109.79
339-Obs 2	21.39	8.26	424.22	110.06
339-Obs 3	21.60	8.16	385.35	109.88
Average	*21.86*	*8.24*	*401.92*	*109.91*
SD	*0.64*	*0.07*	*20.06*	*0.14*
CV%	**2.93**	**0.88**	**4.99**	**0.13**
345-Obs 1	27.81	9.39	391.74	107.86
345-Obs 2	25.62	9.44	398.58	105.16
345-Obs 3	30.15	9.72	391.02	109.45
Average	*27.86*	*9.52*	*393.78*	*107.49*
SD	*2.27*	*0.18*	*4.17*	*2.17*
CV%	**8.13**	**1.87**	**1.06**	**2.02**

Bone resorption parameters were measured in the vertebral body of the 5th lumbar vertebra of 9-week old C57/Bl6 mice. Sections were stained for TRAP with an aniline blue counterstain, imaged at a resolution of 1.4 μm and analysed using TrapHisto. Two samples (339-01 and 345-01) were first analysed on three separate days by a single operator (intra-observer results) and subsequently by three different operators (inter-observer measurements). Oc.S/BS: osteoclast surface per bone surface; N.Oc/BS: number of osteoclasts per bone surface; N.Oc/BV: number of osteoclasts per bone volume; N.Oc/TV: number of osteoclasts per tissue volume, CV: coefficient of variance, SD: standard deviation.

Table 2
OsteoidHisto, reproducibility of measurements.

	BV/TV	BS/BV	Tb.Th	OS/BS	OV/BV	O.Th
Observer 1	%	mm-1	μm	%	%	μm
VK-VG-01	22.11	19.09	110.03	36.99	4.77	9.88
VK-VG-01	22.03	19.18	108.61	29.64	4.02	10.29
VK-VG-01	21.52	19.42	107.56	30.98	4.26	9.93
Average	*21.89*	*19.23*	*108.73*	*32.54*	*4.35*	*10.08*
SD	*0.32*	*0.17*	*1.24*	*3.91*	*0.38*	*0.23*
CV%	**1.46**	**0.89**	**1.14**	**12.03**	**8.80**	**2.24**
VK-VG-03	13.04	12.40	171.04	40.92	5.73	15.23
VK-VG-03	12.97	12.36	170.86	39.64	5.29	15.06
VK-VG-03	13.04	12.41	170.99	41.34	5.75	15.20
Average	*13.02*	*12.39*	*170.96*	*40.63*	*5.59*	*15.16*
SD	*0.04*	*0.03*	*0.09*	*0.89*	*0.26*	*0.09*
CV%	**0.31**	**0.21**	**0.05**	**2.18**	**4.65**	**0.61**
Inter observer						
VK-VG-01-Obs1	21.52	19.42	107.56	30.98	4.26	9.93
VK-VG-01-Obs2	21.96	19.16	107.97	28.25	3.34	8.94
VK-VG-01-Obs3	21.79	19.74	105.15	28.98	3.65	8.87
Average	*21.76*	*19.44*	*106.89*	*29.40*	*3.75*	*9.44*
SD	*0.22*	*0.29*	*1.52*	*1.41*	*0.47*	*0.60*
CV%	**1.02**	**1.49**	**1.43**	**4.81**	**12.48**	**6.31**
VK-VG-03-Obs1	13.04	12.41	170.99	41.34	5.75	15.20
VK-VG-03-Obs2	12.92	12.36	169.39	36.44	4.49	13.28
VK-VG-03-Obs3	12.97	12.38	170.43	35.56	5.22	15.05
Average	*12.98*	*12.38*	*170.27*	*37.78*	*5.15*	*14.24*
SD	*0.06*	*0.03*	*0.81*	*3.11*	*0.63*	*1.07*
CV%	**0.46**	**0.20**	**0.48**	**8.24**	**12.28**	**7.48**

Static bone architecture and osteoid parameters were measured in sections of a human adolescent iliac crest sample. Sections were stained for van Giesson and von Kossa, imaged at a resolution of 1.2 μm and analysed using OsteoidHisto. Two samples (VK-VG-01 and VK-VG-03) were first analysed on three separate days by a single operator (intra-observer results) and subsequently by three different operators (inter- observer measurements). BV/TV: Bone volume per tissue volume; BS/BV: Bone surface per bone volume; Tb.Th: trabecular thickness; OS/BS: osteoid surface per bone surface; OV/BV: osteoid volume per bone volume; O.Th: osteoid thickness, CV: coefficient of variance, SD: standard deviation.

Table 3
CalceinHisto, reproducibility of measurements.

	BV/TV	MAR	MS/BS	BFR/BS
Observer 1	%	μm/day	%	μm³/μm²/day
342-02	27.03	2.92	41.05	1.20
342-02	27.99	2.90	38.92	1.13
342-02	27.58	2.94	45.38	1.34
Average	27.53	2.92	41.78	1.22
SD	0.48	0.02	3.29	0.11
CV%	1.75	0.71	7.88	8.74
388-01	28.77	2.78	40.00	1.11
388-01	28.48	2.82	36.43	1.03
388-01	28.93	2.74	36.28	0.99
Average	*28.73*	*2.78*	*37.57*	*1.04*
SD	*0.23*	*0.04*	*2.11*	*0.06*
CV%	**0.79**	**1.44**	**5.60**	**5.69**
Inter observer				
342-02-Obs1	28.86	3.05	45.05	1.37
342-02-Obs2	27.99	2.90	38.92	1.13
342-02-Obs3	27.34	3.03	38.68	1.17
Average	*28.06*	*2.99*	*40.88*	*1.22*
SD	*0.76*	*0.08*	*3.61*	*0.13*
CV%	**2.72**	**2.61**	**8.83**	**10.51**
388-01-Obs1	28.54	2.61	39.01	1.02
388-01-Obs2	28.48	2.82	36.43	1.03
388-01-Obs3	28.81	2.81	31.58	0.89
Average	*28.61*	*2.75*	*35.67*	*0.98*
SD	*0.18*	*0.11*	*3.77*	*0.08*
CV%	**0.61**	**4.16**	**10.57**	**7.97**

Bone calcein double label parameters were measured in the vertebral body of the 5th lumbar vertebra of 9-week old C57/bl6 mice. Mice were labelled with calcein as described in the method section. Sections were counterstained with calcein blue, imaged at a resolution of 0.3 μm and analysed using CalceinHisto. Two samples (342-02 and 388-01) were first analysed on three separate days by a single operator (intra-observer results) and subsequently by three different operators (inter-observer measurements).
BV/TV: Bone volume per tissue volume; MAR: mineral apposition rate; MS/BS: mineralising surface per bone surface; BFR/BS: bone formation rate per bone surface; CV: coefficient of variance, SD: standard deviation. MS is calculated as the double label surface plus 0.5× single labelled surface. The BFR/BS is calculated as the product of the MAR and MS/BS.

come with a minimum of 8GB of RAM, and should therefore be able to run the software. Several of the imaging functions have been optimised for multithreading and therefore benefit from multicore processors. On quad core processors such as the Intel Core i5-6500 this can lead to a 3-fold reduction in the calculation time of osteoid thickness and double label width. Currently a system with such a processor, 8GB of RAM and a high quality 24″ monitor can be purchased for less than £1000.

As the software was developed using Java, the programs should also run on Apple Macintosh and Linux systems although this has not been tested. The minimum version of Java required is version 7. However, version 7 requires the use of start-up scripts to ensure that Java reserves a sufficient amount of RAM for the analysis. Version 8 of Java dynamically allocates RAM and therefore obviates the need for start-up scripts and the programs can be started directly by double clicking the ".jar" files.

Methods for histomorphometric analysis implemented within general image analysis packages such as ImageJ or commercial packages such as image Pro plus can easily confuse end users through the myriad of functions available and the relatively complex user interface. The software presented here is relatively easy to use as it is designed for a single analysis task and shields the user from most of the complexities of the image analysis. In our experience, a user can easily be trained within an hour, as was observer 3 (LR) in the inter-observer variance tests. As the source code is freely available, users with the required programming experience can extend and optimise the programs to suit their own requirements. It is hoped that the procedures and software presented here will prove useful to the research community and that any improvements made will be fed back into the community.

Table 4
Comparison of TrapHisto, OsteoidHisto and CalceinHisto with Bioquant Osteo.

TrapHisto comparison:

	BV mm²	BV/TV %	TV mm²	BS mm	BS/BV mm⁻¹	Oc.S mm	Oc.S/BS %	Tb.Th μm
Bioquant	0.78	15.26	2.91	37.79	21.83	7.07	18.71	91.62
TrapHisto	0.8	15.73	2.84	37.03	22.59	6.49	17.53	91.75
% difference	*2.56*	*3.08*	*2.41*	*2.01*	*3.48*	*8.20*	*−6.31*	*0.14*

OsteoidHisto comparison:

	OV mm²	OV/BV %	OV/TV %	BV/TV %	BS mm	OS mm	OS/BS %	O.Th μm
Bioquant	0.070	2.58	0.39	26.86	50.43	10.16	20.15	4.69
OsteoidHisto	0.086	3.03	0.47	28.17	52.27	13.2	25.25	7.33
% difference	*22.86*	*17.44*	*21.09*	*4.87*	*3.65*	*29.92*	*25.31*	*56.18*

CalceinHisto comparison:

	BV mm²	BV/TV %	TV mm²	BS mm	MS/BS %	MAR μm/day	BFR/BS μm³/μm²/day
Bioquant	0.29	28.59	1.01	10.13	31.84	1.23	0.39
CalceinHisto	0.29	28.39	1.03	12.7	29.56	1.71	0.51
% difference	*0.00*	*−0.70*	*1.98*	*25.37*	*−6.94*	*39.02*	*30.77*

Images were analysed using the ImageJ based programs and Bioquant Osteo and the results compared. To reduce analysis time for Bioquant Osteo, the images were cropped to the centre part of the original images. The images used were: 339-01 for the resorption parameters, VK-VG-01 for osteoid analysis, and 388-01 for calcein double label analysis.
BV: Bone volume; TV: tissue volume; BV/TV: Bone volume per tissue volume; BS: Bone surface; Oc.S/BS: osteoclast surface per bone surface; Oc.S: osteoclast surface; BS/BV: Bone surface per bone volume; OS: osteoid surface; OS/BS: osteoid surface per bone surface; O.Th: osteoid thickness; Tb.Th: trabecular thickness.
OV: osteoid volume; OV/BV: osteoid volume per bone volume; OV/TV: osteoid volume per tissue volume; BV/TV: Bone volume per tissue volume; BS: Bone surface; OS: osteoid surface; OS/BS: osteoid surface per bone surface; O.Th: osteoid thickness;
MS/BS: mineralising surface per bone surface; MAR: mineral apposition rate; BFR/BS: bone formation rate per bone surface.

References

[1] C.A. Schneider, W.S. Rasband, K.W. Eliceiri, NIH image to ImageJ: 25 years of image analysis, Nat. Methods 9 (2012) 671–675.

[2] A.M. Parfitt, et al., Bone histomorphometry: standardization of nomenclature, symbols, and units: report of the ASBMR Histomorphometry Nomenclature Committee, J. Bone Miner. Res. 2 (1987) 595–610.

[3] D.W. Dempster, et al., Standardized nomenclature, symbols, and units for bone histomorphometry: a 2012 update of the report of the ASBMR Histomorphometry Nomenclature Committee, J. Bone Miner. Res. 28 (2013) 2–17.

[4] R.G. Erben, Bone-labeling techniques, in: Y.H. An, K.L. Martin (Eds.), Handbook of Histology Methods for Bone and Cartilage, Humana Press, Totowa 2003, pp. 99–117.

[5] E. Kinning, et al., An unbalanced rearrangement of chromosomes 4:20 is associated with childhood osteoporosis and reduced caspase-3 levels, J. Pediatr. Genet. 5 (2016) 167–173.

[6] D. Chappard, C. Alexandre, G. Riffat, Histochemical identification of osteoclasts. Review of current methods and reappraisal of a simple procedure for routine diagnosis on undecalcified human iliac bone biopsies, Basic Appl. Histochem. 27 (1983) 75–85.

[7] S. Preibisch, S. Saalfeld, P. Tomancak, Globally optimal stitching of tiled 3D microscopic image acquisitions, Bioinformatics 25 (2009) 1463–1465.

[8] I. Arganda-Carreras, R. Fernandez-Gonzalez, A. Munoz-Barrutia, C. Ortiz-De-Solorzano, 3D reconstruction of histological sections: application to mammary gland tissue, Microsc. Res. Tech. 73 (2010) 1019–1029.

[9] T. Hildebrand, P. Rüesgsegger, A new method for the model-independent assessment of thickness in three-dimensional images, J. Microsc. 185 (1996) 67–75.

[10] R. Juvin, X. Phelip, E. Camus, Y. Usson, An automatic method for bone histomorphometry: assessment with reference to usual static and dynamic parameters, J. Bone Miner. Res. 5 (1990) 235–244.

[11] K.L. Bell, N. Garrahan, M. Kneissel, N. Loveridge, E. Grau, M. Stanton, J. Reeve, Cortical and cancellous bone in the human femoral neck: evaluation of an interactive image analysis system, Bone 19 (1996) 541–548.

[12] X.Y. Tong, et al., Development of new criteria for cortical bone histomorphometry in femoral neck: intra- and inter-observer reproducibility, J. Bone Miner. Metab. 33 (2015) 109–118.